Journal of Solid State Chemistry 182 (2009) 1109–1114

Contents lists available at ScienceDirect

Journal of Solid State Chemistry

journal homepage: www.elsevier.com/locate/jssc

Coupled Li^{1+}/Nb^{5+} and O^{2-}/F^{-} ordering on the Na and Cl sites of the average NaCl structure of Li_4NbO_4F

Lasse Norén [a], Ray L. Withers [a,*], Darren J. Goossens [a], Margaret Elcombe [b], Gordon J. Kearley [b]

[a] Research School of Chemistry, The Australian National University, Canberra, ACT 0200, Australia
[b] Bragg Institute, Building 87, Australian Nuclear Science and Technology Organisation, PMB, Menai, NSW 2234, Australia

ARTICLE INFO

Article history:
Received 3 December 2008
Received in revised form
19 January 2009
Accepted 6 February 2009
Available online 21 February 2009

Keywords:
Disordered metal oxyfluoride
Structured diffuse scattering
Local crystal chemistry
Coupled neutron and X-ray powder diffraction
DFT calculation
Bond valence sum calculation

ABSTRACT

The average, as well as the cation and anion 'disordered', crystal structure of Li_4NbO_4F has been carefully investigated via coupled neutron and X-ray powder diffraction studies as well as via electron diffraction studies. The existence of a spectacular highly structured diffuse intensity distribution in the latter provides strong evidence for coupled Li^{1+}/Nb^{5+} and O^{2-}/F^{-} ordering on the Na and Cl sites of the average NaCl structure of Li_4NbO_4F. Bond valence sum calculations have been used to investigate local crystal chemistry as well as to suggest plausible local crystal chemical constraints while *ab initio* DFT based theoretical calculations of a $2\times2\times2$ supercell have been carried out in order to provide additional insight into the local crystal chemistry of this compound.

1. Introduction

The cubic NaCl-type structure (space group $Fm\bar{3}m$ with both Na^+ and Cl^- ions on special Wyckoff positions at 4*a* (0,0,0) and 4*b* ($\frac{1}{2},\frac{1}{2},\frac{1}{2}$) respectively, see Fig. 1) is very common among ionic compounds such as the alkali halides and the transition metal chalcogenides (see e.g. Table III, 1 of [1]). It also occurs for various inherently non-stoichiometric, solid solution phases such as the rare earth doped sulfide solid solution phases [2], the so-called Hägg phases, e.g. VC_{1-x}, TiN_{1-x} etc. [3,4], as well as for stoichiometric (as far as the cation to anion ratio is concerned) but cation 'disordered' compounds such as e.g. $LiFe^{III}O_2$ [5,6]. Understanding of the local atomic arrangements and associated structural relaxations in such 'disordered' systems provides important insight into the properties of such systems, e.g. into the excellent colour characteristics of the rare earth doped sulfide solid solution phases [2] or the polar behaviour of metal oxyfluoride compounds [7], as well as being of fundamental crystal chemical importance.

In the case of the latter 'disordered' phases, careful diffraction studies sensitive to the weak features of reciprocal space has revealed the presence of a highly structured diffuse intensity distribution in addition to the strong Bragg reflections of an NaCl-type average structure [2,4–8]. Highly structured diffuse distributions are characteristic of many apparently 'disordered' solid solution phases [2,4–11] and contain a great deal of information as to the nature of the local 'order' in such systems but are often by no means a simple matter to interpret [2–12]. In the case of the Hägg phases as well as $Li^+Fe^{3+}O_2$, a complex but quite characteristic, highly structured diffuse intensity distribution was eventually able to be satisfactorily described and explained in terms of important local crystal chemical ordering rules [5,8,9].

Over the years a number of other 'disordered' compounds have also been reported to crystallize with a NaCl-type average structure, in particular the oxyfluoride compound Li_4NbO_4F [13,14] (and related compounds such as Li_3TiO_3F), but without much effort either to search for evidence of local short range ordering or to interpret any such evidence in terms of local ordering rules. Given growing interest in the synthesis and physical properties of mixed anion compounds [15,16] as well as our own recent experiences in the local structural characterization of a range of nominally 'disordered' metal oxyfluoride compounds [17–19], it was decided to re-investigate both the average, as well as the 'disordered', crystal structure of Li_4NbO_4F via coupled neutron and X-ray powder diffraction (XRPD) studies as well as electron diffraction (ED) studies of structured diffuse scattering. Bond valence sum as well as *ab initio* DFT based theoretical calculations were also carried out in order to provide additional insight into the local crystal chemistry of this compound.

* Corresponding author. Fax: +61-2-6125-0750.
E-mail address: withers@rsc.anu.edu.au (R.L. Withers).

0022-4596/$ - see front matter © 2009 Elsevier Inc. All rights reserved.
doi:10.1016/j.jssc.2009.02.015

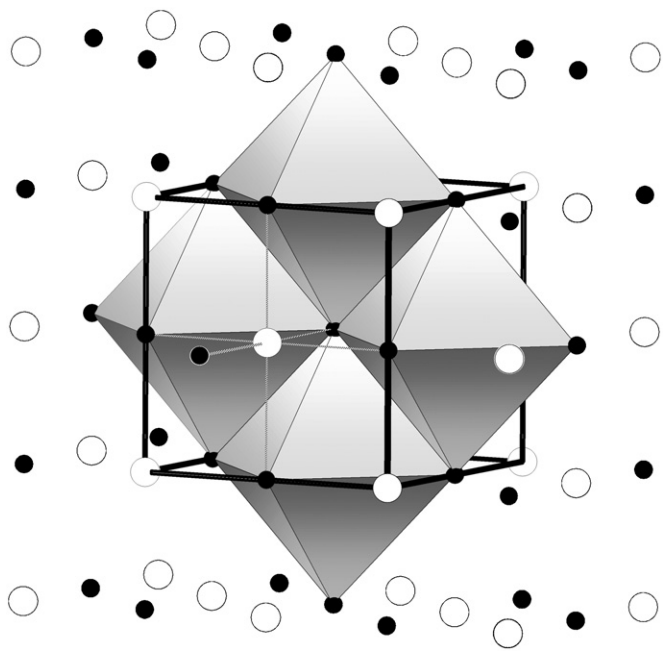

Fig. 1. Illustration of the NaCl structure type. The larger white balls represent the Na^+ ions while the smaller black balls represent the Cl^- ions. Both atom types are octahedrally co-ordinated to the other atom type and the overall structure is formed by edge sharing octahedra of one type (here Cl_6 octahedra). The unit cell is shown by the dark lines.

2. Experimental

2.1. Synthesis

Li_3NbO_4 was first made by grinding dried Li_2CO_3 (3N) and Nb_2O_5 (4N) together in a mortar, pressing to pellets and reacting at 950 °C in air for 24 h [20]. Li_4NbO_4F was then made by grinding together stoichiometric amounts of LiF and Li_3NbO_4, pressing to pellets and heating at 800 °C as well as 1000 °C in air [13,14]. An initial synthesis was attempted to make a reduced lithium niobium(IV) oxyfluoride, $Li_3Nb^{IV}O_3F$ by mixing LiF, Li_2O and with $Nb^{IV}O_2$ (obtained by reducing Nb_2O_5 in flowing H_2 at 800 °C) in vacuum at various temperatures. The result, however, was always the formation of a mix of $Li_4Nb^{V}O_4F$ and $LiNb^{III}O_2$ [21]. Pure $LiNbO_2$ was made following the approach by Kumada et al. [22] by reacting stoichiometric amounts of Li_3NbO_4 with pre-made $Nb^{II}O$ in evacuated silica tubes at 1050 °C for four days. Li_3TiO_3F was synthesised from Li_2CO_3 (3N), TiO_2 (4N) and LiF following the same route as for Li_4NbO_4F [13,14].

2.2. Characterisation

2.2.1. X-ray powder diffraction

The cubic unit cell parameters of the Li_4NbO_4F compound was initially determined via the Guinier–Hägg camera technique using Cu$K_{\alpha 1}$ radiation. High purity silicon powder (Sietronics GD#1 [23]) was used as an internal standard and the program Unitcell [24] was used to refine the unit cell parameters. For average structure refinement purposes, a high intensity X-ray powder pattern was collected using a Panalytical X'Pert Pro X-ray Diffractometer with an X'celerator high speed detector. The radiation used was CuK_{α} and the data was collected over a $5.013° < 2\theta < 142.986°$ range with a step size of 0.033° (see Fig. 2b).

2.2.2. Neutron powder diffraction (NPD)

NPD data was collected over an $0.027° < 2\theta < 150.027°$ range in 0.050° steps using a wavelength of 1.4918 Å on the high resolution powder diffractometer (HRPD) at HIFAR at the Lucas Heights Science and Technology Centre of the Australian Nuclear Science and Technology Organization (ANSTO) (see Fig. 2a).

2.2.3. Electron diffraction

ED data were collected on a Philips EM 430 transmission electron microscope (TEM) operating at 300 kV and a range of different incident orientations.

3. Experimental results

3.1. Average structure refinement results using NPD and XRPD

As Li^+ is an extremely weak scatterer of X-rays, it was initially expected that the neutron data would contain significantly more information on the Li^+ ions. For neutrons, however, the negative scattering length of $4Li^+$ ions (of −7.60 fm) almost exactly cancels out the contribution of the single Nb^{5+} ion (of +7.054 fm) ensuring that the neutron data is dominated by the O^{2-} and F^- anion contributions so that the observed intensities in the neutron data are typical of only one atom per primitive unit cell. For the X-ray data, on the other hand, the average number of electrons on the $\frac{1}{5}$(4Li+1Nb) average cation site is 8.8 while that on the $\frac{1}{5}$(4O+1F) average anion site is 10.0 so that the (h+k+l) odd Bragg reflections of the average NaCl structure type are very weak relative to the (h+k+l) even Bragg reflections in the XRD data (see Fig. 2b). This low scattering factor difference between the cation and anion substructures makes subtle differences difficult to pick up in the X-ray powder pattern.

In order to attempt to overcome these problems, the model was refined against both patterns simultaneously using the program JANA2006 [25]. The background, peak shapes, zero points and scale factors were individually refined against each pattern while the structural parameters were refined against both patterns simultaneously. Two excluded regions were also added: 5.013°–28° for the X-ray pattern and 0.027°–8° for the neutron powder pattern. The undistorted NaCl-type average structure gave a good fit to both patterns (GoF(neutrons/X-rays) = 1.21/1.19, R_p (neutrons/X-rays) = 6.77/1.35, R_{wp} (neutrons/X-rays) = 8.83/1.72, GoF(combined) = 1.20, R_p(combined) = 1.52 R_{wp}(combined) = 2.30). The only structural parameters varied were the a-axis dimension (4.18747(5) Å) and the isotropic atomic displacement parameters (ADPs). In the latter case of the ADPs, it was found that the cation ADPs could be refined independently while the ADPs for the anions could not and were thus constrained to be equal: $U_{iso(4a)} * 100 = 2.26(4)$ Å^2 for Nb and 2.05(5) Å^2 for Li and $U_{iso(4b)} * 100 = 1.08(3)$ Å^2 for O/F. Note that the average structure refinement thus requires that the cations are rather more locally displaced off their ideal positions than are the anions. The final resultant neutron and XRD profiles are shown in Fig. 2a and b, respectively.

The $LiNb^{III}O_2$ sample was also investigated via neutron powder, as well as electron, diffraction. Despite its chemical similarity to $LiFe^{III}O_2$, no indication for cation disorder could be found while the average structure refined from the NPD data was in good agreement with the existing literature [21] and hence is not reported here.

3.2. ED results

Electron diffraction patterns (EDPs) were collected at a wide range of different incident orientations, both exactly on, as well as

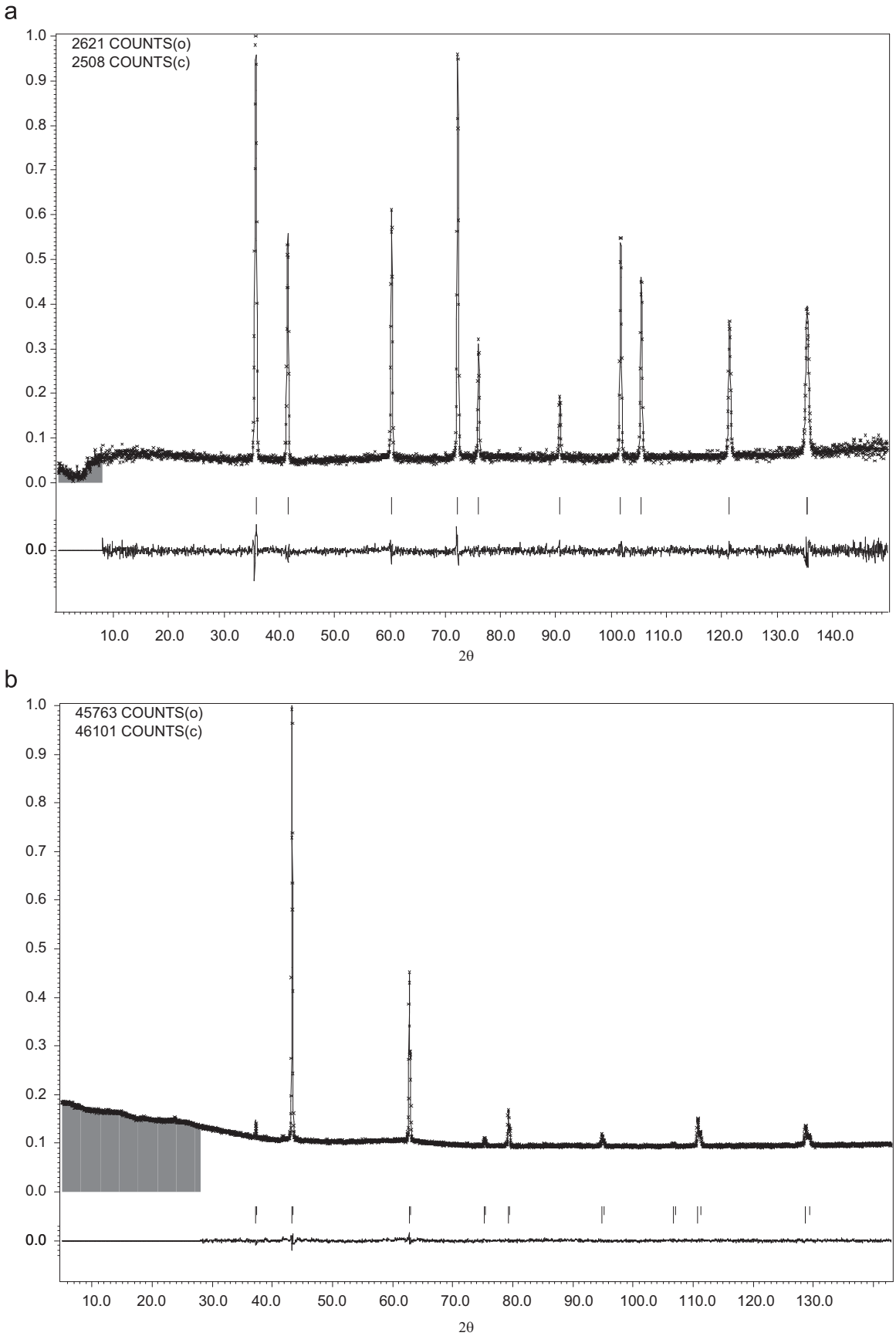

Fig. 2. The observed (a) neutron and (b) X-ray powder diffraction patterns of Li_4NbO_4F along with the calculated patterns given by the solid lines at the top of the figures. The positions of all possible reflections are shown underneath by tick marks while the difference between the observed and the calculated pattern is shown at the bottom of the figures.

close to, many different zone axis orientations. A highly structured, weak but quite reproducible, diffuse intensity distribution was apparent in these EDPs. Figs. 3a–f, for example, show (a) ⟨1,−1,0⟩, (b) ⟨001⟩, (c) ⟨2,−1,0⟩, (d) ⟨1,1,−4⟩, (e) ⟨−2,1,3⟩ and (f) ⟨221⟩ zone axis EDPs typical of Li_4NbO_4F. Very similar EDPs were also obtained for Li_3TiO_3F suggesting that the 'rules' governing the local crystal chemistry of this compound have much in common with those governing the crystal chemistry of Li_4NbO_4F. The existence of such a characteristic, highly structured diffuse intensity distribution shows that both Li_4NbO_4F and Li_3TiO_3F are very far from 'randomly' ordered but rather there must exist strong local rules governing the ordering of the Li^+/Nb^{5+} ions on the cation sub-structure as well as the coupled ordering (and associated structural relaxation) of the O^{2-}/F^- ions on the anion sub-structure.

As mentioned above, however, it is by no means an easy matter to describe let alone interpret such an observed diffuse distribution [4,6,12]. Despite concerted efforts over a several year period using a Monte Carlo based approach in conjunction with reasonable local crystal chemical rules (see below), we have to date been unsuccessful in attempting to describe either the 3-D shape of the observed diffuse distribution in reciprocal space let alone simulate the local ordering rules and associated structural relaxation responsible.

4. Theoretical results

4.1. The bond valence sum approach

In an initial attempt to obtain an understanding of the local crystal chemistry ultimately responsible for the observed structured diffuse scattering apparent in Fig. 3, a bond valence sum [26,27] analysis of the refined average structure ($Fm\bar{3}m$; cation at 0 0 0, anion at $\frac{1}{2}, \frac{1}{2}, \frac{1}{2}$; $a = 4.18747(5)$ Å) was first carried out, the results of which are listed in Table 1.

It is immediately apparent that the calculated bond valence sum, or apparent valence (AV), of the anion is rather more sensitively dependent on the stoichiometry of the surrounding $Li^+_{6-x}Nb^{5+}_x$ octahedral co-ordination polyhedron than the AV of the cation is to the stoichiometry of its surrounding $O^{2-}_{6-x}F^-_x$ octahedral co-ordination polyhedron. The calculated AV of the O^{2-}/F^- anion, for example, is calculated to be only 1.593/1.236 valence units (vus) for a surrounding octahedral co-ordination polyhedral stoichiometry of Li_5Nb but 1.957/1.646 vus for an octahedral co-ordination polyhedral stoichiometry of Li_4Nb_2. This suggests that one might expect the distribution of local octahedral co-ordination stoichiometries surrounding the anions to be rather more tightly bunched close to the average $Li^+_{4.8}Nb^{5+}_{1.2}$ stoichiometry than a random distribution of Li^+ and Nb^{5+} ions might suggest. This would seem to provide the first extremely reasonable local crystal chemical constraint that one might expect to be obeyed.

Notice also that the O^{2-} anion tends to be ~18% under-bonded taking into account the most likely local octahedral co-ordination stoichiometries whereas the F^- anion tends to be ~32% over-bonded (see Table 1). As was also found for FeOF [17], NbO_2F [18] and $K_3MoO_3F_3$ [19], this strongly suggests that F^- anions will prefer to be sited opposite O^{2-} anions in local $O^{2-}_{6-x}F^-_x$ octahedral co-ordination polyhedra so that the centreing cation can move away from the over-bonded F^- anions and towards the under-bonded O^{2-} anions to relieve local crystal chemical strain. This would seem to provide a second extremely reasonable local crystal chemical constraint that one might expect to be obeyed.

By contrast with the above behaviour of the anion AVs, the AV of the Li^+/Nb^{5+} cation, is calculated to be 1.056/3.604 vus for an octahedral co-ordination polyhedral stoichiometry of O_5F_1 and gives very similar calculated AVs of 1.010/3.540 vus for an octahedral co-ordination polyhedral stoichiometry of O_4F_2 so that one would not necessarily expect the distribution of local octahedral co-ordination stoichiometries surrounding the cations to be as tightly bunched close to the average stoichiometry. Note, however, that the Nb^{5+} is heavily under-bonded whatever the local octahedral anion stoichiometry e.g. the highest possible value for the Nb ion AV is 3.668 assuming an O_6 surrounding octahedral stoichiometry. Given that both the Nb^{5+} and O^{2-} ions are, in general, significantly under-bonded if on the ideal NaCl-type positions, one should expect them to mutually attract each other on the local scale whenever possible so as to improve the significant under-bonding of both ions (see Table 1). This appears to provide a third possible ordering principle that one might also expect to be followed.

Serious Monte Carlo based attempts have been made to generate plausible 3-D distributions of locally ordered Li^+/Nb^{5+} and O^{2-}/F^- ions based on the above principles on a large enough scale to enable Fourier transformation for comparison with the EDPs shown in Fig. 3. As mentioned above, however, such an approach has to date failed to generate EDPs that look like those shown in Fig. 3.

4.2. An ab initio density functional theory (DFT) approach

An alternative (*ab initio* DFT) theoretical approach has thus also been employed in order to see what more can be learnt about the local crystal chemistry in such materials as well as to test the above bond valence sum derived expectations. A severe limitation of this approach in a case like this, however, is that a much more limited number of ions can be included in the calculation so that one cannot expect such a calculation to be anywhere near large enough to calculate diffraction patterns for comparison with Fig. 3.

A larger $2 \times 2 \times 2$ supercell was used for the DFT calculations containing 32 cation and 32 anion sites. Each crystallographic site in this array was then filled randomly with either Li or Nb (on the cation sub-structure sites) or O or F (on the anion sub-structure sites) in such a way that the resultant overall stoichiometry was as close as possible to the required Li_4NbO_4F stoichiometry and that cyclic boundary conditions were obeyed. $P1$ space group symmetry for the overall array was then assumed and the ions allowed to relax away from their ideal average structure positions in such a way as to minimize the total energy of the overall array.

The Vienna *ab initio* simulation package, VASP [28], was used for the energy minimization. The effect of the core electrons was simulated by use of an appropriate pseudo-potential while the bonding electrons were modelled via the use of plane waves. The energy cut-off for the plane-wave basis-set was 600 eV and the break-condition for the self-consistent electronic loop was set at 10^{-6} eV. Two K-points were used. A quasi-Newton method was chosen to relax the atomic positions to the energy minima with the break-condition set at 10–5 eV. These characteristics represent good accuracy for both the electronic and structural minimizations that resulted in smooth optimisations of the structure, usually with 20 cycles. Two such simulations were carried out. The first had $26Li^+$ and $6Nb^{5+}$ ions occupying the cation sub-structure and $24O^{2-}$ and $8F^-$ anions occupying the anion sub-structure and was thus charge balanced. The second simulation had $26Li^+$ and $6Nb^{5+}$ ions occupying the cation sub-structure and $25O^{2-}$ and $7F^-$ anions occupying the anion sub-structure and thus had one excess electron. The results obtained from the two simulations, however, were quite similar.

Fig. 4a shows a histogram plot of the number of ions that were displaced from the ideal NaCl-type positions as a fraction of the

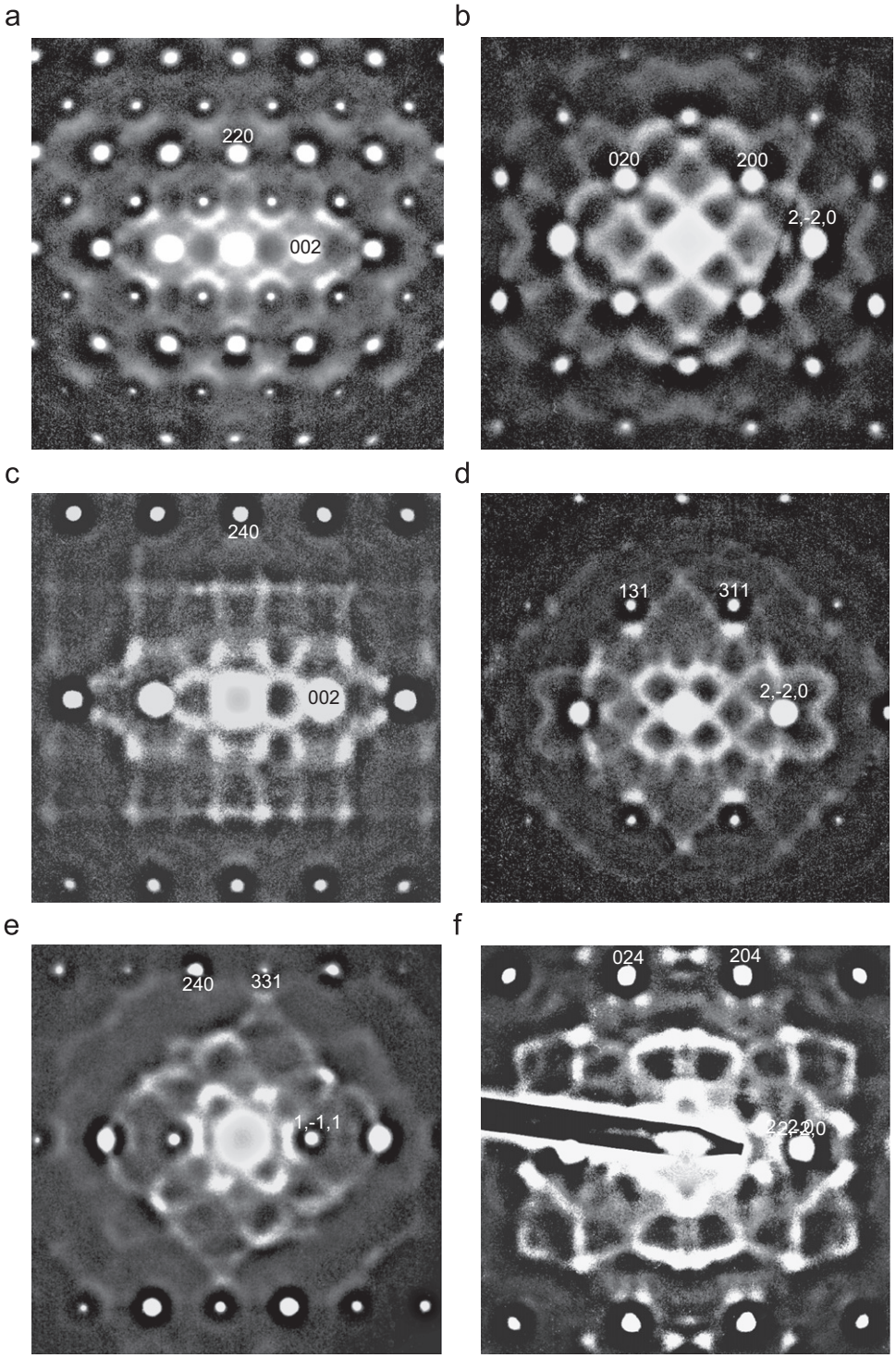

Fig. 3. (a) ⟨1,−1,0⟩, (b) ⟨001⟩, (c) ⟨2,−1,0⟩, (d) ⟨1,1,−4⟩, (e) ⟨−2,1,3⟩ and (f) ⟨221⟩ zone axis EDPs typical of Li_4NbO_4F.

magnitude of the displacement expressed in fractions of the supercell dimension, $2a = 8.375$ Å, for the sum of both simulations. Each histogram bar has a width of ± 0.003 fractional units. Note that the O^{2-} and F^- anions are found to displace significantly less than the Li^+ and Nb^{5+} cations, in agreement with the refined average structure ADPs. While the displacements of the anions can be modelled as an ADP, those of the cations cannot. The cations are displaced significantly from their average positions. Fig. 4b shows the various cation–anion bond lengths obtained, again as a fraction of the supercell dimension. (The distribution of the Li–O bond lengths is excluded from Fig. 4b as there are rather more of them, relatively speaking, and their inclusion confuses the histogram). Note that the average Nb^{5+}–O^{2-} bond length is significantly less than the mean bond length value of 0.25 (as is also predicted by the bond valence sum approach) while both the Nb^{5+}–F^- and Li^+–F^- average bond lengths are significantly longer than 0.25.

The average AV and the standard deviation thereof (in brackets) for the two simulations was 1.065(0.084) for the Li^+ ions, 4.452(0.142) for the Nb^{5+} ions, −1.897(0.153) for the O^{2-} ions

Table 1
Apparent valences (AVs) of the ions in Li_4NbO_4F calculated assuming the ideal NaCl-structure type and for all possible local co-ordination environments.

	Li_6	Li_5Nb	Li_4Nb_2	Li_3Nb_3	Li_2Nb_4	$LiNb_5$	Nb_6	Average
AV(O)	1.102	1.593	1.957	2.385	2.813	3.240	3.668	1.637
AV(F)	0.827	1.236	1.646	2.055	2.464	2.874	3.283	1.316
	O_6	O_5F	O_4F_2	O_3F_3	O_2F_4	OF_5	F_6	
AV(Li)	1.102	1.056	1.010	0.965	0.919	0.873	0.827	1.046
AV(Nb)	3.668	3.604	3.540	3.476	3.411	3.347	3.283	3.588
P	0.262	0.393	0.246	0.082	0.015	0.001	0.000	

The probability (*P*) weighted averaged AV of each ion is given in the last column. $0.8Li_5Nb+0.2Li_4Nb_2 = Li_{4.8}Nb_{1.2}$.

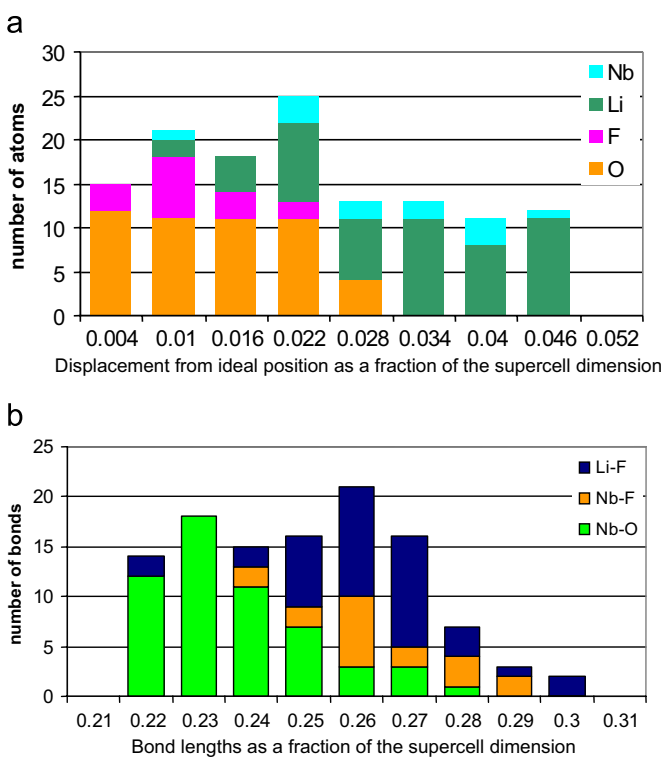

Fig. 4. (a) A histogram plot of the number of ions displaced from the ideal NaCl-type positions as a fraction of the magnitude of the displacement (expressed in fractions of the supercell dimension, $2a = 8.375$ Å) for the sum of both simulations. Each histogram bar has a width of ± 0.003 fractional units. (b) The various cation–anion bond lengths obtained, again as a fraction of the supercell dimension. The Li–O bond lengths have been omitted for the purposes of clarity.

and $-1.112(0.142)$ vus for the F^- ions. Clearly the AV of the Nb ion has improved significantly (although it still remains significantly under-bonded, cf. Table 1) as a result of the relaxations introduced. Likewise the AVs of the O^{2-} and F^- ions have also improved noticeably (again cf. with Table 1) while that of the Li ion is also reasonable. The major drawback of the *ab initio* calculation approach, however, the assumed initial random ordering, remains and hence so does the problem of fitting to, and understanding the origin of, the observed highly structured diffuse intensity distribution.

5. Conclusions

The average, as well as the cation and anion 'disordered', crystal structure of Li_4NbO_4F has been carefully determined via coupled neutron and X-ray powder diffraction studies. The significantly larger ADPs on the cation sites is consistent with the results of *ab initio* DFT calculations of a $2 \times 2 \times 2$ supercell array. Bond valence sum calculations have been used to suggest plausible local crystal chemical constraints. Nb and O ions will clearly move towards one another on the local scale while Nb and F ions as well as Li and F ions will tend to move apart. It remains to understand the coupled Li^{1+}/Nb^{5+} and O^{2-}/F^- ordering on the Na and Cl sites of the average NaCl-structure type implied by the existence of a spectacular, highly structured diffuse intensity distribution apparent in EDPs of Li_4NbO_4F.

Acknowledgments

We acknowledge the support of the Australian Institute for Nuclear Science and Engineering (AINSE) for financial support through grant AINGRA062250. R.L.W. and D.J.G. acknowledge the support of the Australian Research Council (ARC) in the form of ARC Discovery Grants. D.J.G. thanks AINSE for financial support in the form of an AINSE Fellowship.

References

[1] R.W.G. Wyckoff, Crystal Structures, vol. 1, second ed., Krieger, Malabar, Florida, USA
[2] R.L. Withers, E. Urones-Garrote, L. Carlos Otero-Díaz, Phil. Mag. 87 (2007) 2807–2813.
[3] G. Hägg, Teknisk Tidskrift Bergsvetenskap 61 (1931) 23–26.
[4] J. Billingham, P.S. Bell, M.H. Lewis, Acta Crystallogr. A 28 (1972) 602–606.
[5] M. Brunel, F. De Bergevin, M. Gondrand, J. Phys. Chem. Solids 33 (1972) 1927–1941.
[6] J.M. Cowley, Acta Crystallogr. A 29 (1973) 537–540.
[7] R.L. Withers, F.J. Brink, Y. Liu, L. Norén, Polyhedron 26 (2007) 290–299.
[8] M. Sauvage, E. Parthé, Acta Crystallogr. A 28 (1972) 607–616.
[9] R. de Ridder, D. van Dyck, G. van Tendeloo, S. Amelinckx, Phys. Status Solidi A 40 (1977) 669–683.
[10] R.L. Withers, J.G. Thompson, P.J. Barlow, J. Solid State Chem. 94 (1991) 89–105.
[11] T.R. Welberry, R.L. Withers, Phys. Chem. Miner. 17 (1990) 117–124.
[12] R.L. Withers, Solid State Sci. 5 (2003) 115–123.
[13] A.I. Agulyanskii, V.A. Bessonova, V.Ya. Kuznetsov, V.T. Kalinnikov, Russ. J. Inorg. Chem. 29 (1984) 613–614.
[14] A.I. Agulyanskii, V.A. Bessonova, V.Ya. Kuznetsov, V.T. Kalinnikov, Russ. J. Inorg. Chem. 31 (1986) 1547–1548.
[15] T. Katsumata, M. Nakashima, H. Umemoto, Y. Inaguma, J. Solid State Chem. 181 (2008) 2737–2740.
[16] S.J. Clarke, P. Adamson, S.J.C. Herkelrath, O.J. Rutt, D.R. Parker, M.J. Pitcher, C.F. Smura, Inorg. Chem. 47 (2008) 8473–8486.
[17] F.J. Brink, R.L. Withers, J.G. Thompson, J. Solid State Chem. 155 (2000) 359–365.
[18] F.J. Brink, R.L. Withers, L. Norén, J. Solid State Chem. 166 (2002) 73–80.
[19] F.J. Brink, R.L. Withers, K. Friese, G. Madariaga, L. Norén, J. Solid State Chem. 163 (2002) 267–274.
[20] G. Blasse, Z. Anorg. Allg. Chem. 326 (1963) 44–46.
[21] G. Meyer, R. Hoppe, Angew. Chem. Int. Ed. 13 (1974) 744–745.
[22] N. Kumada, S. Muramatu, F. Muto, N. Kinomura, S. Kikkawa, M. Koizumi, J. Solid State Chem. 73 (1988) 33–39.
[23] Sietronics Pty Ltd., Unit 3/22, Walder St., Belconnen, ACT 2612, Australia.
[24] B. Noläng, Ben Systems, Örnsätra, SE-74022 Bälinge, Sweden.
[25] V. Petrícek, M. Dušek, L. Palatinus, JANA2006, The Crystallographic Computing System Institute of Physics, Praha, Czech Republic, 2006.
[26] I.D. Brown, The Chemical Bond in Inorganic Chemistry. The Bond Valence Method, Oxford University Press, Oxford, 2002.
[27] M. O'Keeffe, N.E. Brese, Acta Crystallogr. B 47 (1991) 192–197.
[28] G. Kresse, J. Furthmüller, Software VASP, Vienna, 1999.